International Journal for Multidisciplinary Research (IJFMR)

E-ISSN: 2582-2160 ● Website: www.ijfmr.com ● Email: editor@ijfmr.com

Impact of Thermal Radiation, Dufour Effects, and Chemical Reaction on Oscillatory MHD Flow Through Porous Media

A. Sinha

Department of Mathematics, Y.S. Palpara Mahavidyalaya, Palpara Purba Medinipur, West Bengal, India-721458

Abstract

In this study, the effects of the Dufour number and the heat generation parameter on magneto-hydrodynamic (MHD) free convection flow of an electrically conducting, incompressible viscous fluid past an inclined plate embedded in a porous medium are investigated. The analysis considers an impulsively started plate with variable surface temperature and mass diffusion. By employing a closed-form analytical approach, the dimensionless momentum, energy, and mass diffusion equations are solved to obtain exact expressions for the velocity, temperature, and concentration fields. These solutions are shown to reduce to several previously reported results in the literature as special cases, while satisfying all prescribed initial and boundary conditions. Furthermore, analytical expressions for the skin friction coefficient, Nusselt number, and Sherwood number are derived. The influence of key parameters on velocity, temperature, and concentration distributions, as well as on heat and mass transfer characteristics, is illustrated graphically and discussed in detail.

Keywords: MHD, Porous Medium, Thermal Radiation, Chemical reaction, Dufour effect, Skin friction coefficient.

Introduction

Over the past several decades, significant attention has been devoted to the study of heat and mass transfer in magneto-hydrodynamic (MHD) flow over an inclined plate, particularly within the fields of hypersonic aerodynamics, astrophysics, and renewable energy systems. In various real-world scenarios, including chemical reactions, evaporation, and condensation, the mass transfer process invariably precedes the heat transfer process. For this reason, understanding a variety of technical transfer processes can be facilitated by studying combined heat and mass transfer. The MHD conjugative heat transfer problem from vertical surfaces immersed in saturated porous media was formulated and analysed by Duwairi and Al-Kablawi [1]. Seddeek[2] examined how a changing magnetic field and viscosity affected the flow and heat transfer via a porous plate that was moving continuously. The effects of mass transfer on a continuous two-dimensional laminar MHD mixed convection flow were studied by Abdelkhalek [3]. In thermal convection, the heat source/sink effects are important in situations when the surface (such as the spacecraft body) and the surrounding fluid may have considerable temperature differences. In the context of an exothermic or endothermic chemical reaction, heat generation is equally significant. The effects of radiation, heat generation, and viscous dissipation on MHD free convection flow along a stretching sheet have been studied by Tania et al. [4]. Moreover, Moalem[5] investigated the impact of temperature-dependent heat sources on heat transmission in a porous material during electrical heating. The hydro magnetic convection at a cone and a wedge in the presence of temperature-dependent heat generation or absorption effects was reported by Vajravelu and Nayfeh [6]. Additionally, Chamkha[7] investigated the impact of heat generation or absorption on a vertical stretched surface hydro magnetic three-dimensional free convection flow. Shankar et al. [8] investigated the effects of radiation and mass transfer on MHD free convection fluid flow immersed in a porous media with heat generation/absorption. The Dufour effect is the name given to the heat transfer brought on by the concentration gradient. Numerous researchers have examined the Dufour effects. The thermo-diffusion and diffusion-thermo effects on the combined free-forced convective and mass transfer of steady laminar boundary layer flow over a vertical flat were investigated by Kafoussias and Williams [9]. In a Darcy porous medium with chemical reactions and heat generation, Mohamad[10] investigated the Soret effect on the unsteady magnetohydrodynamics (MHD) free convection heat and mass transfer flow over a semi-infinite vertical plate.. The free convective heat and mass transport of an incompressible electrically conducting fluid over a stretching sheet in the presence of injection and suction with the Soret and Dufour effects was investigated numerically by Afify [11]. The Soret effect on oscillatory MHD free convective flow via a vertical porous plate in slip flow regime with chemical reaction and radiation was investigated by Islam and Ahmed [12].Postelnicu[13] used the Darcy Boussinesq model in the presence of Dufour and Soret effects to study the simultaneous heat and mass transfer by natural convection from a vertical flat plate embedded in an electrically-conducting fluid saturated porous medium. The Soret and Dufour effects on mixed convection unsteady MHD boundary layer flow over stretching sheet in a porous media containing chemically reactive species were examined by Nayak et al. [14].

Due to the aforementioned studies, we have examined in this paper an analytical solution of an MHD free convection flow with heat and mass transfer phenomena that will be of interest to researchers in the fields of geophysics, astrophysics, electrochemistry, and polymer processing as well as the engineering community. The flow over an inclined porous medium in the presence of heat and mass transfer as well as a uniform magnetic field applied in a direction normal to the sheet has been examined in this paper along with the effects of Dufour, chemical reaction, and thermal radiation of an electrically conducting viscous incompressible fluid.

Formulation of the Problem

Let us analyze the unsteady behavior of an incompressible viscous fluid flowing past an infinite inclined plate under the influence of variable heat and mass transfer. The x'-axis is taken along the plate with the angle of inclination α to the vertical and the y'-axis is taken normal to the plate. The viscous fluid is taken to be electrically conducting and fills the porous half space $y'>0$. A uniform magnetic field of strength B_0 is applied in the y'-direction transversely to the plate. Due to the aforementioned studies, we have examined in this paper an analytical solution of an MHD free convection flow with heat and mass transfer phenomena that will be of interest to researchers in the fields of geophysics, astrophysics, electrochemistry, and polymer processing as well as the engineering community. The flow over an inclined porous medium in the presence of heat and mass transfer as well as a uniform magnetic field applied in a direction normal to the sheet has been examined in this paper along with the effects of Dufour, chemical reaction, and thermal radiation of an electrically conducting viscous incompressible fluid. Initially, both the fluid and the plate are at rest with constant temperature T_∞ and constant concentrationC_∞. At time t'>0, the plate is jerked abruptly, causing motion in the direction of flow against gravity with uniform velocity u_0. The temperature and concentration of the plate increase linearly with time. It is also assumed that viscous dissipation is negligible, and that the fluid is a thick grey medium that absorbs and emits radiation but scatters none. Since the plate is infinite in the (x', z') plane, all physical variables are functions of y' and t' only. The physical model and coordinates system is shown in Fig. 1.

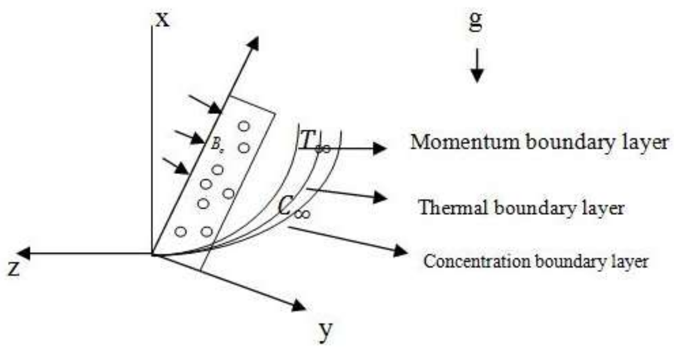

Fig. 1: Physical model of the problem

Given the aforementioned assumptions and the standard Boussinesq approximation, the governing equations reduce to

$$\frac{\partial u'}{\partial t'} = \nu\frac{\partial^2 u'}{\partial y'^2} + g\beta(T - T_\infty)\cos\alpha + g\beta_c(C - C_\infty)\cos\alpha - \frac{\sigma B_0{}^2}{\rho}u' - \frac{\nu}{K^*}u' \quad (1)$$

$$\frac{\partial T}{\partial t'} = \frac{\kappa}{\rho C_p}\frac{\partial^2 T}{\partial y'^2} - \frac{1}{\rho C_p}\frac{\partial q'}{\partial y'} + \rho\frac{D_M K_T}{C_s}\frac{\partial^2 C}{\partial y'^2} \quad (2)$$

$$\frac{\partial C}{\partial t'} = D_M\frac{\partial^2 C}{\partial y'^2} - K_1(C - C_\infty) \quad (3)$$

The boundary conditions are

$$t' \le 0: u' = 0, T = T_\infty, C = C_\infty \qquad for\ all\ y' > 0$$
$$t' > 0\ :\ \ u' = U_0, T = T_\infty + (T_w - T_\infty)At',\ \ C = C_\infty + (C_w - C_\infty)At' \qquad at\ y' = 0$$
$$u' = 0, T = T_\infty, C = C_\infty \qquad as\ y' \to \infty \quad (4)$$

We adopt the Rosseland approximation for radiative heat flux q_r, namely

$$q' = -\frac{4\sigma^*}{3a^*}\frac{\partial T^4}{\partial y'} \quad (5)$$

Now expanding T^4 in Taylor series about T_∞ and neglecting higher order terms

$$T^4 \cong 4TT_\infty^3 - 3T_\infty^4 \quad (6)$$

To normalize the equations (1)-(3) the following non-dimensional quantities are introduced.

$$u = \frac{u'}{U_0}, t = \frac{t'U_0{}^2}{\nu}, y = \frac{y'U_0}{\nu}, \theta = \frac{T - T_\infty}{T_W - T_\infty}, \varphi = \frac{C - C_\infty}{C_W - C_\infty} \quad (7)$$

The non-dimensional form of the equations (1), (2) and (3) are as follows

$$\frac{\partial u}{\partial t} = \frac{\partial^2 u}{\partial y^2} + Gr\theta\cos\alpha + Gm\varphi\cos\alpha - (M + \frac{1}{K})u \quad (8)$$

$$\frac{\partial\theta}{\partial t} = \frac{1+N}{Pr}\frac{\partial^2\theta}{\partial y^2} - \frac{N\theta}{Pr} - \frac{Q}{Pr}\theta + D_u\frac{\partial^2\varphi}{\partial y^2} \quad (9)$$

$$\frac{\partial\varphi}{\partial t} = \frac{1}{Sc}\frac{\partial^2\varphi}{\partial y^2} - K\varphi \tag{10}$$

The corresponding non dimensional boundary conditions are

$$t \le 0: \quad u = 0, \theta = 0, \varphi = 0 \qquad for\ all\ y > 0$$
$$t > 0 \ : \quad u = 1, \theta = t, \varphi = t \qquad at\ y = 0$$
$$u \to 0, \theta \to t, \varphi \to t \qquad as\ y \to \infty \tag{11}$$

In order to normalize the mathematical model, we introduce the following non-dimensional quantifies

$$Gr = \frac{\nu g\beta(T_w - T_\infty)}{{U_0}^3}\ , Gm = \frac{\nu g\beta^*(C_w - C_\infty)}{{U_0}^3}\ , Pr = \frac{\mu c_p}{\boldsymbol{\kappa}}\ , K^* = \frac{a^*{U_0}^2}{\nu^2}\ , Sc = \frac{\nu}{D_M}\ ,$$
$$M = \frac{\sigma{B_0}^2\nu}{\rho{U_0}^2}, K = \frac{K_1\nu}{{U_0}^2}\ , N = \frac{16\sigma{T_\infty}^3}{3\kappa a^*}\ , Q = \frac{\gamma^2 Q\prime}{K{U_0}^2}\ , D_u = \frac{D_T K_T(C_w - C_\infty)}{\gamma C_p C_s(T_w - T_\infty)} \tag{12}$$

Method of solution

Consider the velocity field u, temperature distribution θ, concentration profile φ as follows:

$$u = u_0 e^{-\omega t}$$
$$\theta = \theta_0 e^{-\omega t}$$
$$\varphi = \varphi_0 e^{-\omega t} \tag{13}$$

On substitution of (13), in equations (8), (9), and (10), we get

$$u_0'' - {a_3}^2 u_0 = -(Gr\theta_0 + Gm\varphi_0)\cos\alpha \tag{14}$$
$$\theta_0'' - {a_2}^2\theta_0 = D_u\varphi_0'' \tag{15}$$
$$\varphi_0'' - {a_1}^2\varphi_0 = 0 \tag{16}$$

The corresponding boundary conditions become:

$$u_0 = e^{-\omega t}\ , \quad \theta_0 = te^{-\omega t}\ , \quad \varphi_0 = \grave{}te^{-\omega t} \quad at\ y = 0$$
$$u_0 \to 0\ ,\ \theta_0 \to 0\ ,\ \varphi_0 \to 0 \quad as\ y \to \infty \tag{17}$$

The analytical solutions of the equations (14) to (16) subject to the boundary condition (17) are

$$\varphi_0 = te^{-\omega t}e^{-a_1 t} \tag{18}$$
$$\theta_0 = te^{-\omega t}e^{-a_2 t} - \frac{a_3}{({a_1}^2 - {a_2}^2)}e^{-(a_1+a_2)y} + \frac{a_3}{({a_1}^2 - {a_2}^2)}e^{-a_1 y} \tag{19}$$
$$u_0 = e^{-\omega t}e^{-a_4 t} - a_{10}e^{-(a_4+a_2)y} - a_{11}e^{-(a_4+a_2+a_1)y} - a_{12}e^{-(a_4+a_1)y} + a_{10}e^{-a_2 y} + a_{11}e^{-(a_1+a_2)y} + a_{12}e^{-a_1 y} \tag{20}$$

In view of the above solutions, the velocity, temperature and concentration distribution in the boundary layer become:

$$u = e^{-a_4 t} - a_{10}e^{-(a_4+a_2)y+\omega t} - a_{11}e^{-(a_4+a_2+a_1)y+\omega t} - a_{12}e^{-(a_4+a_1)y+\omega t} + a_{10}e^{-a_2 y+\omega t} + a_{11}e^{-(a_1+a_2)y+\omega t} + a_{12}e^{-a_1 y+\omega t} \tag{21}$$

$$\theta = te^{-a_2 t} - \frac{a_3}{\left(a_1^2 - a_2^2\right)}e^{-(a_1+a_2)y+\omega t} + \frac{a_3}{\left(a_1^2 - a_2^2\right)}e^{-a_1 y+\omega t} \tag{22}$$

And

$$\varphi = te^{-a_1 t}e^{\omega t} \tag{23}$$

Skin friction

The non-dimensional form of skin friction coefficient at plate is given by

$$\tau = e^{-a_4 t} + a_{10}\left(a_4 + a_2\right)e^{\omega t} + a_{11}\left(a_4 + a_2 + a_1\right)e^{\omega t} + a_{12}\left(a_4 + a_1\right)e^{\omega t}$$
$$- a_{10}a_2 e^{\omega t} - a_{11}\left(a_1 + a_2\right)e^{\omega t} - a_1 a_{12} e^{\omega t} \qquad (24)$$

Nusselt Number

$$Nu = -a_2 t + \frac{a_3\left(a_1 + a_2\right)}{\left(a_1^2 - a_1^2\right)}e^{\omega t} + \frac{a_3 a_1}{\left(a_1^2 - a_1^2\right)}e^{\omega t} \qquad (25)$$

Sherwood Number

$$Sh = -a_1 t \qquad (26)$$

Results and discussion

To gain a physical understanding of the issue, we investigated the impact of parameters such as Hartmann number, heat source parameter, radiation parameter, Dufour number, Schmidt number, thermal Grashof number, Prandtl number, and permeability parameter on velocity field, temperature profile, concentration distribution, and skin friction at the plate (figure 2-18), while keeping other parameters constant. Figure 2 shows how raising the magnetic field strength affects the thickness of the momentum boundary layer. It is now generally understood that the magnetic field has a damping effect on the velocity field by producing drag force that opposes fluid motion, causing the velocity to decrease. Figures 3 and 13 show that while velocity declines, temperature increases. Physically, this is correct since more radiation happens when the temperature rises, and as a result, the velocity increases. Figure 4 depicts how the Dufour number affects the velocity boundary layer. The thickness of the velocity boundary layer is shown to rise with an increase in the Dufour number. The impact of the Schmidt number on velocity is shown in Figure 5. It is observed that the velocity field increases with increasing Schmidt number. The impact of the thermal Grashof number on the velocity field is shown in Figure 6. The relationship between the thermal buoyant force and the viscous hydrodynamic force is indicated by the thermal Grashof number. The increase in buoyant force that results from a rise in the thermal Grashof number accelerates the flow. Figure 7 illustrates how velocity profiles are affected by dimensionless time. A growing function of time is found for velocity. The fluid velocity trend near the vertical plate is shown in Figure 8 and is slightly higher when the Prandtl number increases.

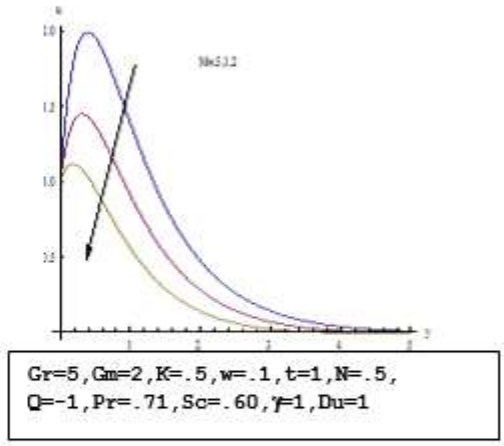

Fig 2: Velocity Distribution for different Values of M

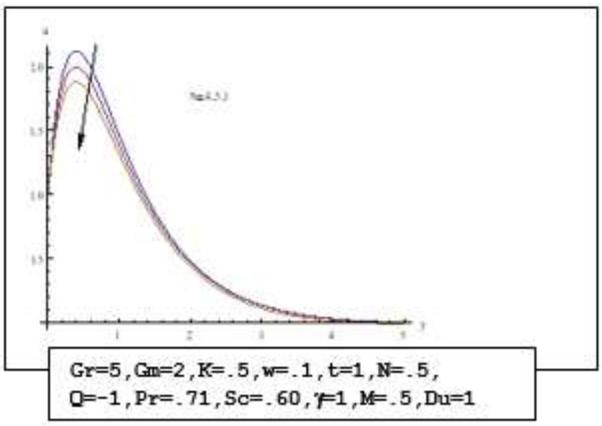

Fig 3: Velocity Distribution for different Values of N

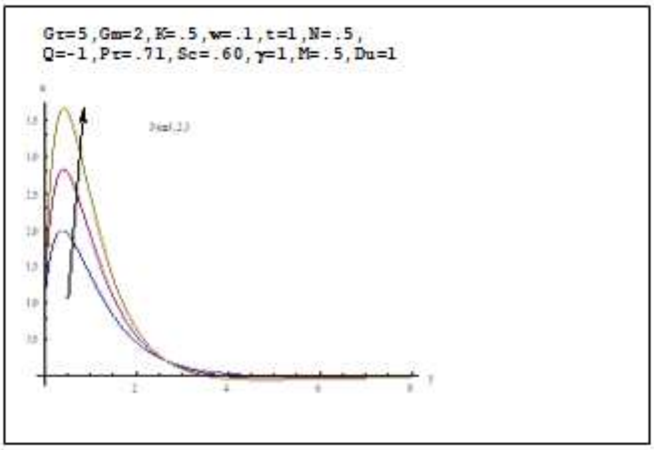

Fig 4: Velocity Distribution for different Values of Du

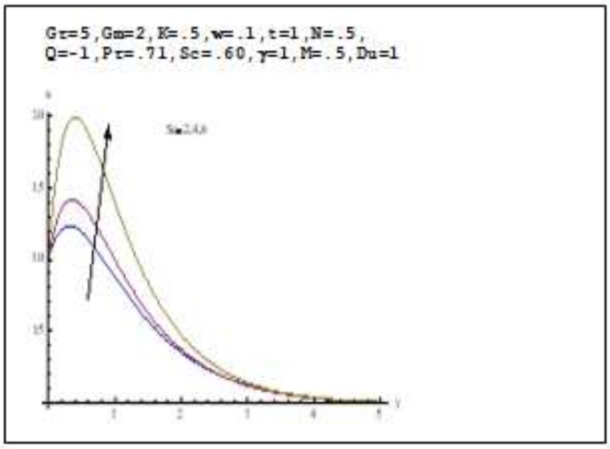

Fig 5: Velocity Distribution for different Values of Sc

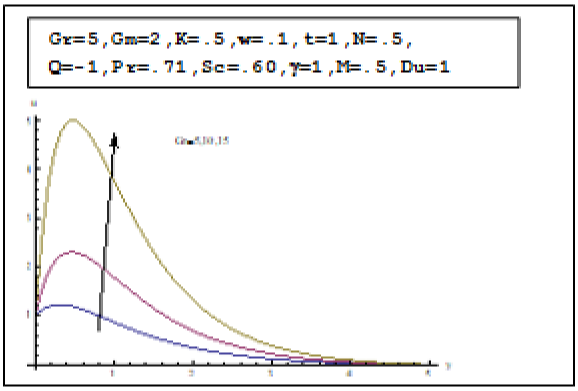

Fig 6: Velocity Distribution for different Values of Gr

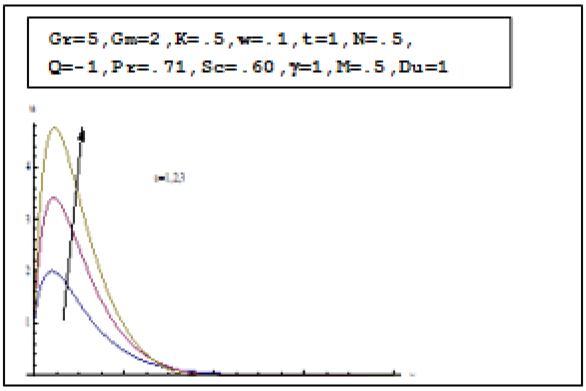

Fig 7: Velocity Distribution at different times

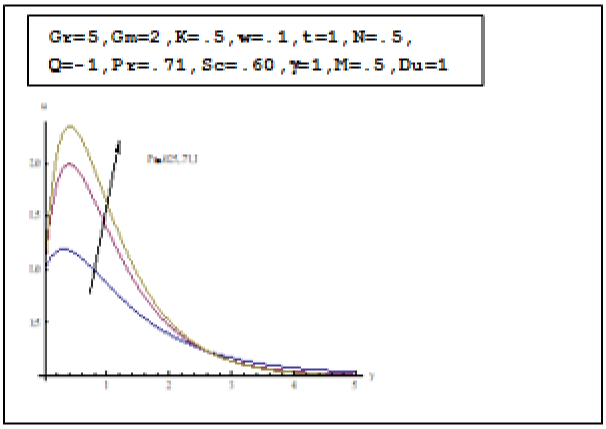

Fig 8: Velocity Distribution for different Values of Pr

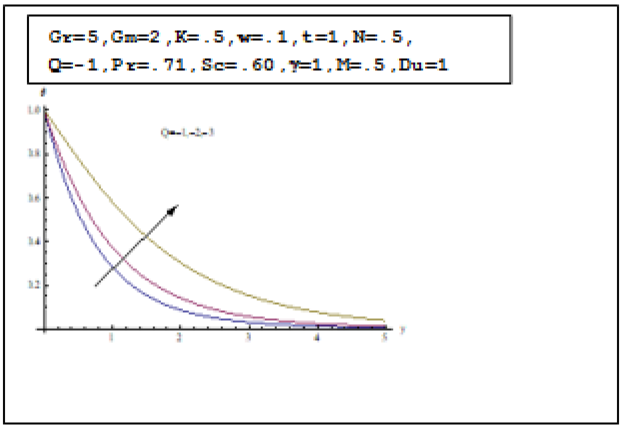

Fig 9: Temperature Distribution for different Values of Q

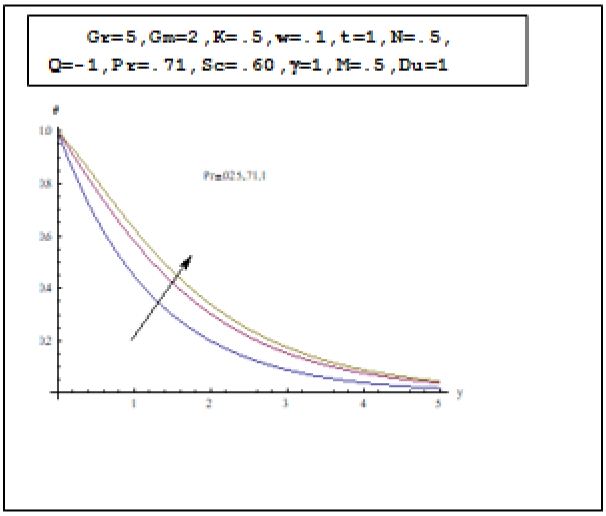

Fig 10: Temperature Distribution for different Values of Pr

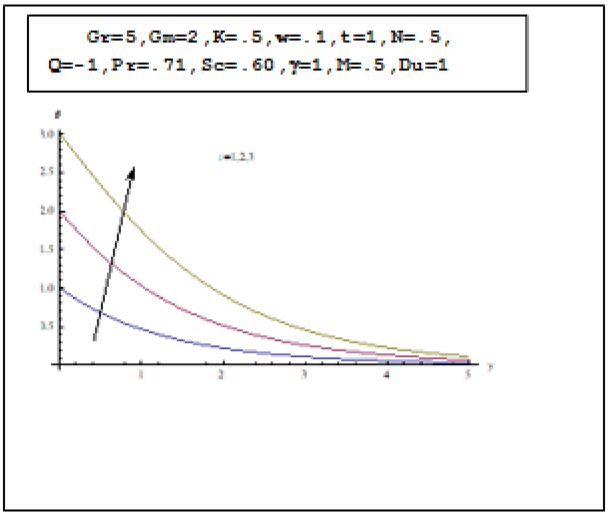

Fig 11: Temperature Distribution at different times

Heat generation/absorption parameter effects on temperature are shown in Figure 9. The temperature is found to grow in direct proportion to the heat generation/absorption parameter. The impact of the Prandtl number on temperature is shown in Figure 10. It is observed that temperature rises with increasing Prandtl number. Plotting of the effects of the dimensionless time t on the temperature is presented in Figure 11. It goes without saying that as time passes, the temperature rises. Equation (11) provides a boundary condition for the temperature field,

. As a result, the accuracy is verified, and we are certain that the temperature analytical result is accurate. The thermal boundary-layer variation with the Dufour number is depicted in Figure 12. It is observed that as the Dufour number rises, so does the thickness of the thermal boundary layer. Additionally, as illustrated in figure 13, the temperature profiles for rising radiation parameter values demonstrate an increasing behavior. Since the radiation parameter indicates the proportional contribution of conduction heat transfer to thermal radiation transmission, a similar behavior is also anticipated. The physical consequence of the chemical reaction parameter is depicted in Figure 14, which amply illustrates how concentration profiles rapidly decline when K is increased. The impact of Schmidt number on concentration is shown in Figure 15. It is observed that the concentration field tends to decrease as the Schmidt number rises.

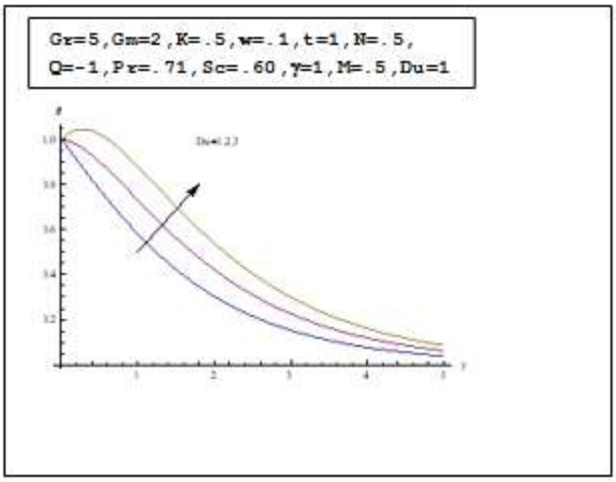

Fig 12: Temperature Distribution for different Values of Du

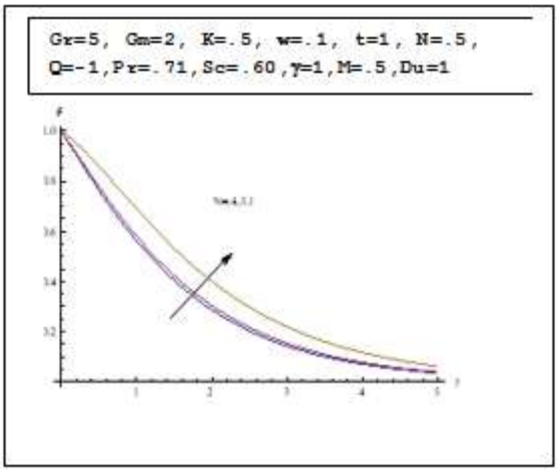

Fig 13: Temperature Distribution for different Values of N

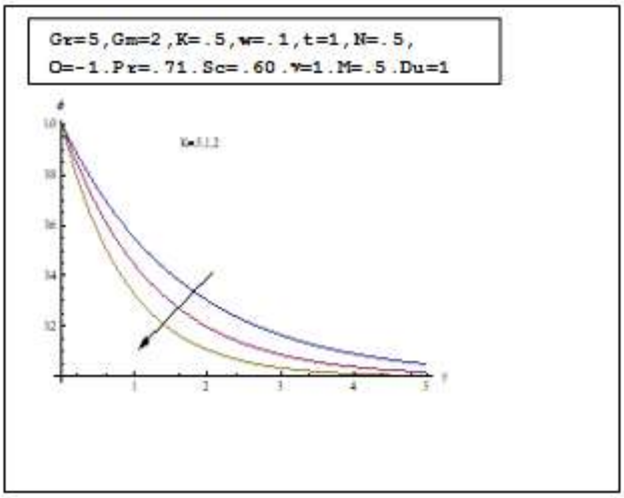

Fig 14: Concentration Profile distribution for different values of K

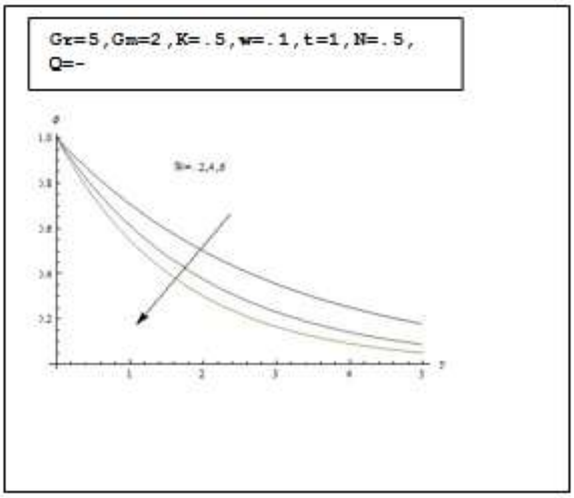

Fig 15: Concentration Profile distribution for different values of Sc

The skin friction variation against t for various values of N, Du, and M is displayed in Figures 16, 17, and 18.It is observed that when Du grows, the local skin-friction coefficient increases, but when N & M increase, it reduces.

Conclusions

In this problem, we examine the effects of a transversely applied magnetic field in the presence of a heat source on a steady MHD mixed convective fluid flow past a continuously moving infinite vertical porous plate. We also examine the effects of a Schmidt number, heat source parameter, thermal Grashof number, radiation parameter, Hartmann number, Soret number, and Prandtl number, as well as chemical reaction. Using the perturbation technique, the non-dimensional governing equations are solved, and the results are shown as graphs.

The following results are drawn from the current investigation:

- The velocity profile reduces with an increase in Hartmann number and increases with thermal radiation, chemical reaction, Prandtl number, and thermal Grashof number.

- Heat source parameter, chemical reaction, and thermal diffusion cause the fluid's temperature to drop.
- The fluid's concentration increases while the Soret effect is at work, but it decreases when a chemical reaction and Schmidt number are at play.
- When thermal radiation, chemical reaction, and thermal Grashof number increase, the generated magnetic field's magnitude reduces, while thermal diffusion's impact causes it to increase.
- The use of a heat-generating source lowers the coefficient of skin friction.

References

1. H. M. Duwairi, Y. Al-Kahlawi, International Journal of Heat and Technology,**24**(1), 123-128, (2006).
2. M. A. Seddeek, Int. Commun Heat Mass, **27**(7), 1037-1046,(2000).
3. M. M. Abdelkhalek, Int. commun Heat Mass, **33**, 249-258, (2006).
4. S. Tania, Khaleque and M. A. Samad, Research J of Appl. Sci., Eng. and Tech,**2(** 4), 368-377, (2010).
5. D. Moalem, Int. J.Heat and Mass Transfer, **19**, 529–537, (1976).
6. K. Vajrevelu, J. Nayfeh, Int. Comm. Heat Mass Transfer, **19**, 701–710, (1992).
7. A. J. Chamkha**,** Int. J. Heat and Fluid Flow,**20**, 84–92, (1999).
8. B. Shankar, B. Prabhakar Reddy, and AnandaRao, Indian Journal of pure and applied physics, **48**, 157-165, (2010).
9. N. G. Kafoussias and E. W. Williams, International Journal of Engineering Science, **33(**9), 1369–1384, (1995).
10. R. A. Mohamad, Applied Mathematical Sciences, **3**(13), 629– 651, (2009).
11. A. Afify, Communications in Nonlinear Science and Numerical Simulation, **14**, (5), 2202–2214,(2009).
12. S. H. Islam, N Ahmed, Journal of the Calcutta Mathematical Society},13(1), 41-58, (2017).
13. A. Postelnicu, International Journal of Heat and Mass Transfer, **47,** 1467-1472,(2004).
14. A. Nayak, S. Panda, and D. K. Phukan, Applied Mathematics and Mechanics, **35**, 849-862,(2014).

Nomenclature

a^* Mean absorption coefficient
B_o Magnitude of applied magnetic field
C Fluid concentration
τ Skin friction coefficient
C_s Concentration susceptibility
C_p Specific heat at constant pressure
D_M Mass diffusivity
D_T Thermal diffusivity
g Acceleration due to gravity
Gm Solutal Grashof number
Gr Thermal Grashof number

K Chemical reaction parameter
K_1 Chemical reaction constant
K^* Permeability parameter
K_T Thermal diffusion ratio
M Hartmannn number
N Radiation parameter
Nu Nusselt number
p Fluid pressure
Pr Prandtl number
$\vec{q}$ Fluid velocity
q' Radiative heat flux
Sc Schmidt number
Sh Sherwood number
Du Duffour number
T Fluid temperature
T_m Mean fluid temperature
T_∞ Fluid temperature in free stream
T_w Fluid temperature at the wall
u' Axial velocity
α Inclination of the plate with the vertical
β Volume expansion coefficient for heat transfer
β^* Volume expansion coefficient for mass transfer
κ Thermal conductivity
μ Coefficient of viscosity
υ Kinematic viscosity
ρ Fluid density
σ Electrical conductivity
σ^* Stefen-Boltzman constant
C_w Dimensional species concentration at the wall,
C_∞ Dimensional species concentration at infinity,
Q Heat source parameter
t' Dimensional time
t Dimensionless time
φ Dimensionless concentration,
θ Dimensionless temperature